Available online at www.sciencedirect.com
SCIENCE DIRECT®
Journal of Sound and Vibration 282 (2005) 401–410
JOURNAL OF SOUND AND VIBRATION
www.elsevier.com/locate/jsvi

Free vibration analysis of membranes using the *h–p* version of the finite element method

A. Houmat*

Department of Mechanical Engineering, Faculty of Engineering, University of Tlemcen, Tlemcen 13000, Algeria

Received 23 September 2003; accepted 25 February 2004
Available online 12 October 2004

Abstract

The *h–p* version of the finite element method is applied to the vibration of membranes. This is accomplished using a polynomially enriched triangular element. New simple expressions of hierarchical C^0 shape functions for triangles are given in terms of the shifted Legendre orthogonal polynomials. The *h–p* version of the finite element method marries both the concepts of the conventional *h*-version and the *p*-version. The accuracy of the solution is sought by simultaneously refining the mesh and increasing the polynomial order in each element. Results of frequency calculations are found for triangular and L-shaped membranes using a number of meshes and polynomial orders. It is shown that the *h–p* version of the finite element method is always convergent from above and produces a high accuracy with few degrees of freedom.

1. Introduction

A membrane is a special case of a plate when tension is the dominating factor and the resistance to bending is very small. There are only a few known exact solutions for the natural frequencies of membranes. Among the exact solutions are those for rectangular, circular, and triangular domains. The reason so few exact solutions exist is that closed-form solutions to vibration problems for irregular domains are difficult to obtain. Thus, approximate methods have to be

*Tel./fax: +213-43-20-15-34.
E-mail address: a_houmat@wissal.dz (A. Houmat).

0022-460X/$ - see front matter © 2004 Elsevier Ltd. All rights reserved.
doi:10.1016/j.jsv.2004.02.042

Nomenclature

x, y	rectangular Cartesian coordinates
ξ_1, ξ_2, ξ_3	non-dimensional area coordinates
t	time
A^e	element surface area
w^e	element transverse displacement
p	polynomial order
ρ	surface density
S	surface tension
$K^e_{m,n}$	element stiffness matrix
$M^e_{m,n}$	element mass matrix
q^e_n	element generalized coordinates
N^e	order of element stiffness and mass matrices
$\mathbf{K}^g$	global stiffness matrix
$\mathbf{M}^g$	global mass matrix
$\mathbf{q}^g$	global generalized coordinates
ω	natural frequency
Ω	$= \omega\sqrt{\rho/S}$, frequency parameter

found. In this context, the *h–p* version of the finite element method is extended to the vibration of membranes.

In the *h–p* version of the finite element method, the error in the solution is controlled by both the diameter h of the largest element and the polynomial order p [1,2]. The *h–p* version of the finite element method has been exploited in a few areas including plate vibrations [3] and beam statics [4] and has been shown to offer considerable savings in computational effort when compared with the standard *h*-version of the finite element method. A previous author's work [5] was concerned with the application of a rectangular *p*-element to membrane vibrations. The present work is the first implementation of the *h–p* version of the finite element method based on a triangular element to the vibration of membranes.

The hierarchical C^0 shape functions for triangles have been first derived by Peano [6]. Szabo and Babuska [7] expressed these functions in terms of the Legendre orthogonal polynomials. In this paper, alternative simpler expressions of the C^0 hierarchical shape functions for triangles are given in terms of the shifted Legendre orthogonal polynomials.

Numerical examples will show that the use of the *h–p* version of the finite element method in membrane vibration problems is valuable. The high accuracy of the solution using a few elements and polynomial orders demonstrates the effectiveness of the method to membrane vibrations.

2. Formulation

2.1. The shape functions

A triangular element is shown in Fig. 1. Also shown in the figure are the dimensionless area coordinates $\xi_1(=1-\xi_2-\xi_3)$, ξ_2, ξ_3 and their nodal and edge values (a list of nomenclature is given).

The C^0 shape functions for triangles $g_n(\xi_1,\xi_2,\xi_3)(n=1,2,3,\ldots,(p+1)(p+2)/2)$ consist of

- Three nodal shape functions:

$$\xi_1, \xi_2, \xi_3, \tag{1}$$

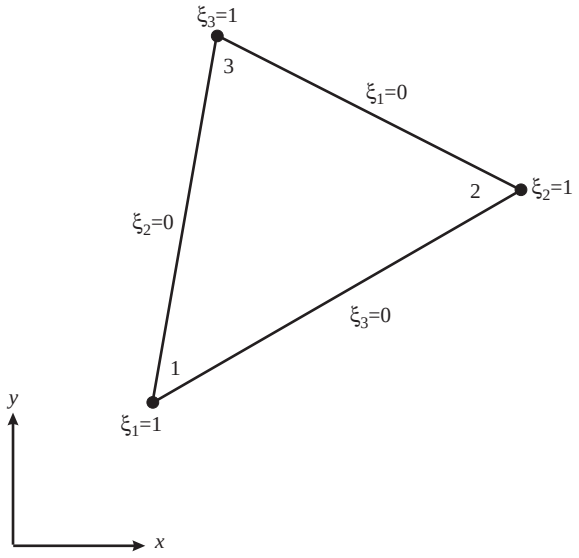

Fig. 1. The triangular element coordinates.

- $(p-1)$ shape functions on edge 1–2:

$$\xi_1\xi_2P_i^*(\xi_2), \tag{2}$$

- $(p-1)$ shape functions on edge 2–3:

$$\xi_2\xi_3P_i^*(\xi_3), \tag{3}$$

- $(p-1)$ shape functions on edge 1–3:

$$\xi_1\xi_3P_i^*(\xi_3), \tag{4}$$

where

$$i = 0, 1, 2, \ldots, p-2, \tag{5}$$

- $(p-1)(p-2)/2$ shape functions in the interior of the element:

$$\xi_1\xi_2\xi_3P_j^*(\xi_2)P_k^*(\xi_3), \tag{6}$$

where

$$j = 0, 1, 2, \ldots, p-3, \tag{7}$$

$$k = p-j-3. \tag{8}$$

In the above, P_r^* denotes the rth order shifted Legendre orthogonal polynomial [8].

The hierarchical C^0 shape functions $g_n(\xi_1, \xi_2, \xi_3)(n = 1, 2, 3, \ldots, 28)$ for $p \leqslant 6$ are quoted explicitly in Table 1. They are given in the order shown in the table to preserve "hierarchy". This property means that the shape functions corresponding to an interpolation of order p constitute a

Table 1
The hierarchical C^0 shape functions for triangles ($p \leqslant 6$)

n	g_n
1	ξ_1
2	ξ_2
3	ξ_3
4	$\xi_1\xi_2$
5	$\xi_2\xi_3$
6	$\xi_1\xi_3$
7	$2\xi_1\xi_2^2 - \xi_1\xi_2$
8	$2\xi_2\xi_3^2 - \xi_2\xi_3$
9	$2\xi_1\xi_3^2 - \xi_1\xi_3$
10	$\xi_1\xi_2\xi_3$
11	$6\xi_1\xi_2^3 - 6\xi_1\xi_2^2 + \xi_1\xi_2$
12	$6\xi_2\xi_3^3 - 6\xi_2\xi_3^2 + \xi_2\xi_3$
13	$6\xi_1\xi_3^3 - 6\xi_1\xi_3^2 + \xi_1\xi_3$
14	$2\xi_1\xi_2^2\xi_3 - \xi_1\xi_2\xi_3$
15	$2\xi_1\xi_2\xi_3^2 - \xi_1\xi_2\xi_3$
16	$20\xi_1\xi_2^4 - 30\xi_1\xi_2^3 + 12\xi_1\xi_2^2 - \xi_1\xi_2$
17	$20\xi_2\xi_3^4 - 30\xi_2\xi_3^3 + 12\xi_2\xi_3^2 - \xi_2\xi_3$
18	$20\xi_1\xi_3^4 - 30\xi_1\xi_3^3 + 12\xi_1\xi_3^2 - \xi_1\xi_3$
19	$4\xi_1\xi_2^2\xi_3^2 - 2\xi_1\xi_2^2\xi_3 - 2\xi_1\xi_2\xi_3^2 + \xi_1\xi_2\xi_3$
20	$6\xi_1\xi_2^3\xi_3 - 6\xi_1\xi_2^2\xi_3 + \xi_1\xi_2\xi_3$
21	$6\xi_1\xi_2\xi_3^3 - 6\xi_1\xi_2\xi_3^2 + \xi_1\xi_2\xi_3$
22	$70\xi_1\xi_2^5 - 140\xi_1\xi_2^4 + 90\xi_1\xi_2^3 - 20\xi_1\xi_2^2 + \xi_1\xi_2$
23	$70\xi_2\xi_3^5 - 140\xi_2\xi_3^4 + 90\xi_2\xi_3^3 - 20\xi_2\xi_3^2 + \xi_2\xi_3$
24	$70\xi_1\xi_3^5 - 140\xi_1\xi_3^4 + 90\xi_1\xi_3^3 - 20\xi_1\xi_3^2 + \xi_1\xi_3$
25	$20\xi_1\xi_2^4\xi_3 - 30\xi_1\xi_2^3\xi_3 + 12\xi_1\xi_2^2\xi_3 - \xi_1\xi_2\xi_3$
26	$20\xi_1\xi_2\xi_3^4 - 30\xi_1\xi_2\xi_3^3 + 12\xi_1\xi_2\xi_3^2 - \xi_1\xi_2\xi_3$
27	$12\xi_1\xi_2^2\xi_3^3 - 12\xi_1\xi_2^2\xi_3^2 + 2\xi_1\xi_2^2\xi_3 - 6\xi_1\xi_2\xi_3^3 + 6\xi_1\xi_2\xi_3^2 - \xi_1\xi_2\xi_3$
28	$12\xi_1\xi_2^3\xi_3^2 - 12\xi_1\xi_2^2\xi_3^2 + 2\xi_1\xi_2\xi_3^2 - 6\xi_1\xi_2^3\xi_3 + 6\xi_1\xi_2^2\xi_3 - \xi_1\xi_2\xi_3$

subset of the set of shape functions corresponding to an interpolation of order $p+1$ and therefore the stiffness and mass matrices of the element of order p are sub-matrices of the stiffness and mass matrices of the element of order $p+1$.

2.2. The p-element stiffness and mass matrices

The potential energy U^e and kinetic energy T^e of the membrane triangular p-element may be expressed as

$$U^e = \frac{S}{4A^e}\int_{A^e}\left[\left(\sum_{l=1}^{3} a_l \frac{\partial w^e}{\partial \xi_l}\right)^2 + \left(\sum_{l=1}^{3} b_l \frac{\partial w^e}{\partial \xi_l}\right)^2\right] \mathrm{d}A, \tag{9}$$

$$T^e = \rho A^e \int_{A^e} (\dot{w}^e)^2 \, \mathrm{d}A, \tag{10}$$

where the dot denotes differentiation with respect to time and the parameters a_l and b_l are defined in terms of the nodal x and y coordinates as

$$a_1 = x_3 - x_2, \quad a_2 = x_1 - x_3, \quad a_3 = x_2 - x_1, \tag{11}$$

$$b_1 = y_2 - y_3, \quad b_2 = y_3 - y_1, \quad b_3 = y_1 - y_2. \tag{12}$$

The transverse displacement w^e in this element may be expressed as

$$w^e = \sum_{n=1}^{N^e} g_n(\xi_1, \xi_2, \xi_3) q_n^e(t). \tag{13}$$

Substituting Eq. (13) into Eqs. (9) and (10) gives

$$U^e = \tfrac{1}{2} q_m^e K_{m,n}^e q_n^e, \tag{14}$$

$$T^e = \tfrac{1}{2} \dot{q}_m^e M_{m,n}^e \dot{q}_n^e, \tag{15}$$

where

$$m = 1, 2, 3, \ldots, N^e. \tag{16}$$

The element stiffness and mass matrices can be expressed as

$$K_{m,n}^e = \frac{S}{2A^e} \sum_{\alpha=1}^{3} \sum_{\beta=1}^{3} (a_\alpha a_\beta + b_\alpha b_\beta) I_{m,n}^{\alpha,\beta}, \tag{17}$$

$$M_{m,n}^e = 2\rho A^e J_{m,n}. \tag{18}$$

The order of the element stiffness and mass matrices is

$$N^e = \tfrac{1}{2}(p+1)(p+2). \tag{19}$$

The integrals are defined as

$$I_{m,n}^{\alpha,\beta} = \int_{A^e} \frac{\mathrm{d}g_m}{\mathrm{d}\xi_\alpha} \frac{\mathrm{d}g_n}{\mathrm{d}\xi_\beta} \, \mathrm{d}A, \tag{20}$$

$$J_{m,n} = \int_{A^e} g_m g_n \, \mathrm{d}A. \tag{21}$$

Each of the above integrals can be put into the following form:

$$\int_0^1 \int_0^{1-\xi_3} f(\xi_2, \xi_3) \, \mathrm{d}\xi_2 \, \mathrm{d}\xi_3. \tag{22}$$

The above integral can be calculated exactly by using symbolic computing which is available through a number of commercial packages.

The integrals required to evaluate the element stiffness and mass matrices up to a maximal value of p equal to 12 were calculated exactly using symbolic computing and stored in a file. During execution, the program opens this file and reads the values of the integrals.

If edge and internal generalized coordinates are regarded as associated with edge and internal fictitious nodes whose number is p-dependent and are assigned numbers in the same way as nodal generalized coordinates, then the assembly process will be identical to its counterpart in the h-version and so the techniques used in the h-version become applicable.

Boundary conditions may be applied during the assembly process simply by ignoring the restrained generalized coordinates.

Assuming harmonic motion, the governing equations of free motion can be obtained by substituting the resultant global stiffness and mass matrices into Lagrange's equations. This yields the following equations:

$$[\mathbf{K}^g - \omega^2 \mathbf{M}^g]\mathbf{q}^g = 0. \tag{23}$$

The solution to the above generalized eigenvalue problem yields the natural frequencies.

3. Results

Two examples were considered to illustrate the convergence and accuracy of the h–p version of the finite element method. The first example is a right isosceles triangular membrane (Fig. 2). One of the reasons for choosing this particular membrane is that natural frequencies can be found in closed form [9] and hence it will provide a basis of comparison for the current method. Results for the 10 lowest frequency parameters Ω are shown in Table 2 along with the exact solution. The results were generated from meshes of 1, 3, and 6 elements (Fig. 3) with $p = 4$, 6, 8, 10, and 12 in each element. In Table 2, NEL and NDOF denote the number of elements in each mesh and the number of degrees of freedom, respectively. It is clearly shown in Table 2 that in each of the three

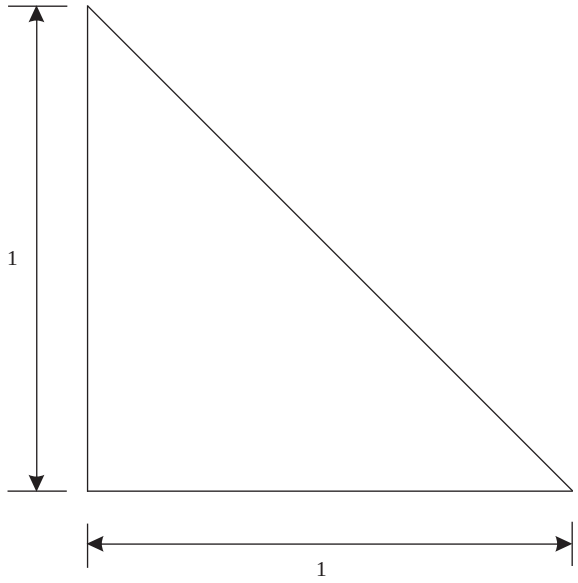

Fig 2. The right isosceles triangular membrane.

Table 2
The 10 lowest frequency parameters Ω of the right isosceles triangular membrane

NEL	p	NDOF	Mode no.									
			1	2	3	4	5	6	7	8	9	10
1	6	10	7.0325	10.0166	11.5580	14.8772	15.9193	16.8263	19.4435	21.1345	23.0694	24.9900
	8	21	7.0249	9.9369	11.3508	13.1091	14.2952	15.9298	16.3966	18.0269	19.7404	21.0900
	10	36	7.0248	9.9346	11.3281	12.9597	14.0674	15.7531	16.0475	17.1589	18.6887	19.8173
	12	55	7.0248	9.9346	11.3272	12.9532	14.0502	15.7123	16.0201	16.9438	18.3760	19.1741
3	4	19	7.0647	10.2957	11.7468	15.0259	15.3207	18.0283	21.4031	23.0740	23.7094	24.4075
	6	46	7.0260	9.9564	11.3727	13.2959	14.2991	15.8947	17.1940	17.9087	19.8653	21.0655
	8	85	7.0248	9.9351	11.3310	12.9826	14.0914	15.7400	16.1660	17.1811	18.6071	20.0647
	10	136	7.0248	9.9346	11.3273	12.9542	14.0525	15.7147	16.0282	16.9709	18.3823	19.2526
	12	199	7.0248	9.9346	11.3272	12.9531	14.0497	15.7086	16.0193	16.9229	18.3274	19.1216
6	4	37	7.0260	9.9928	11.4078	13.2849	14.4433	15.9545	16.5110	18.2242	19.5313	21.2321
	6	91	7.0248	9.9351	11.3294	12.9671	14.0731	15.7224	16.0465	16.9999	18.5004	19.2953
	8	169	7.0248	9.9346	11.3272	12.9533	14.0501	15.7082	16.0197	16.9199	18.3312	19.1200
	10	271	7.0248	9.9346	11.3272	12.9531	14.0496	15.7080	16.0190	16.9180	18.3187	19.1098
	12	397	7.0248	9.9346	11.3272	12.9531	14.0496	15.7080	16.0190	16.9180	18.3185	19.1096
	Exact		7.0248	9.9346	11.3272	12.9531	14.0496	15.7080	16.0190	16.9180	18.3185	19.1096

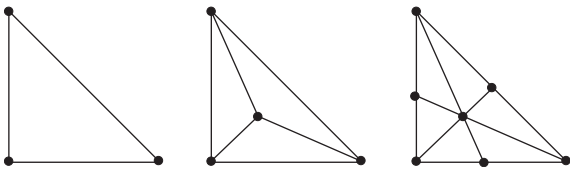

Fig. 3. Meshes for solutions given in Table 2.

models a rapid convergence from above occurs as the polynomial order p is increased from 4 to 12 and highly accurate values are obtained for $p = 12$. The most accurate values are found for the 6-element mesh and $p = 12$ in each element. In fact, these values agree up to 4 significant digits with the exact ones for all of the 10 lowest modes. The reason that this model offers the most accurate values is that it uses the largest number of degrees of freedom (NDOF = 397).

The second example is an L-shaped membrane (Fig. 4). One of the reasons for choosing this particular membrane is that it is one of the most troublesome to solve because of the re-entrant corner which causes difficulty in estimating several of the lower modes. There is no known closed-form solution to this problem but highly accurate solutions are available in the literature [10]. Results for the 10 lowest frequency parameters Ω are shown in Table 3 along with the solution of Fox et al. [10]. The results were generated from meshes of 4, 6, and 12 elements (Fig. 5) with $p = 4$, 6, 8, 10, and 12 in each element. Table 3 clearly shows that in each of the three models

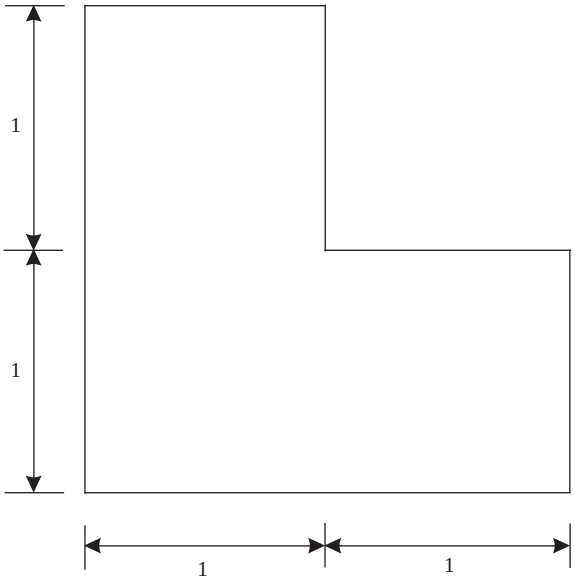

Fig. 4. The L-shaped membrane.

Table 3
The 10 lowest frequency parameters Ω of the L-shaped membrane

NEL	p	NDOF	Mode no.									
			1	2	3	4	5	6	7	8	9	10
4	4	21	3.1272	3.9058	4.4560	5.7714	6.0131	6.8298	7.2595	7.6299	8.3327	9.0610
	6	55	3.1122	3.8988	4.4429	5.4447	5.6765	6.4646	6.7258	7.0658	7.0858	7.6057
	8	105	3.1084	3.8984	4.4429	5.4335	5.6541	6.4435	6.7051	7.0259	7.0261	7.5353
	10	171	3.1068	3.8984	4.4429	5.4334	5.6519	6.4419	6.7044	7.0248	7.0248	7.5323
	12	253	3.1061	3.8984	4.4429	5.4334	5.6508	6.4412	6.7044	7.0248	7.0248	7.5317
6	4	33	3.1170	3.9039	4.4497	5.5249	5.7151	6.6032	7.1284	7.3893	7.4779	8.0216
	6	85	3.1094	3.8985	4.4429	5.4343	5.6564	6.4470	6.7119	7.0383	7.0444	7.5510
	8	161	3.1071	3.8984	4.4429	5.4334	5.6521	6.4421	6.7046	7.0250	7.0250	7.5328
	10	261	3.1061	3.8984	4.4429	5.4334	5.6509	6.4412	6.7044	7.0248	7.0248	7.5317
	12	385	3.1056	3.8984	4.4429	5.4334	5.6502	6.4408	6.7044	7.0248	7.0248	7.5313
12	4	81	3.1123	3.8988	4.4439	5.4382	5.6607	6.4665	6.7457	7.0332	7.0332	7.5579
	6	193	3.1077	3.8984	4.4429	5.4334	5.6531	6.4431	6.7047	7.0248	7.0248	7.5334
	8	353	3.1062	3.8984	4.4429	5.4334	5.6510	6.4413	6.7044	7.0248	7.0248	7.5318
	10	561	3.1056	3.8984	4.4429	5.4334	5.6502	6.4408	6.7044	7.0248	7.0248	7.5313
	12	817	3.1053	3.8984	4.4429	5.4334	5.6498	6.4405	6.7044	7.0248	7.0248	7.5310
Fox et al. [10]			3.1048	3.8983	4.4428	5.4333	5.6492	6.4400	6.7043	7.0248	7.0248	7.5305

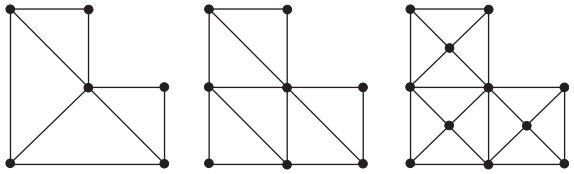

Fig. 5. Meshes for solutions given in Table 3.

Table 4
Comparison of the 10 lowest frequency parameters Ω of the right isosceles triangular membrane

Element type	NDOF	Mode no.									
		1	2	3	4	5	6	7	8	9	10
Triangular p-element	15	7.025	9.984	11.390	13.141	14.698	16.255	19.441	20.483	21.226	21.803
Linear triangular element	15	7.324	10.897	12.522	14.958	16.813	18.504	19.401	21.390	23.350	23.557
Triangular p-element	36	7.025	9.935	11.328	12.960	14.067	15.753	16.048	17.159	18.689	19.817
Linear triangular element	36	7.173	10.412	11.938	13.958	15.493	17.205	17.862	19.374	21.368	22.080
Triangular p-element	55	7.025	9.935	11.327	12.953	14.050	15.712	16.020	16.944	18.376	19.174
Linear triangular element	55	7.128	10.267	11.758	13.651	15.069	16.783	17.307	18.641	20.529	21.229
Exact		7.025	9.935	11.327	12.953	14.050	15.708	16.019	16.918	18.319	19.110

convergence is rapid from above as the polynomial order p increases from 4 to 12 and an excellent agreement with the values of Fox et al. is obtained for $p = 12$. The most accurate values are found for the 12-element mesh and $p = 12$ in each element. This model offers the most accurate values because it uses the largest number of degrees of freedom (NDOF = 817).

The performance of the triangular p-element with that of the linear triangular element on a degree of freedom basis is also investigated. The linear triangular element represents the special case of the triangular p-element when $p = 1$. Results for the 10 lowest modes of the right isosceles triangular membrane are shown in Table 4 along with the exact solution. The results of the p-element were generated from a one-element mesh with $p = 7$, 10, and 12 and NDOF = 15, 36, and 55, respectively. The results of the linear triangular element were generated from meshes of 49, 100, and 144 elements and NDOF = 15, 36, and 55, respectively. Table 4 clearly shows that the p-element produces a higher accuracy that the linear triangular element with fewer degrees of freedom.

It is well known that orthogonal polynomials have the drawback that numerical rounding errors associated with floating point arithmetic increase with increasing polynomial order. In the h–p version of the finite element method, the desired accuracy can be achieved by using a certain number of degrees of freedom. This can be accomplished using two different procedures. The first procedure consists of fixing the mesh and increasing the polynomial order. This is known as the p-version of the finite element method. The second procedure consists of fixing the polynomial order below its critical value and refining the mesh. The latter procedure has the advantage over the

former in that it is capable of avoiding numerical rounding errors associated with floating point arithmetic.

4. Conclusion

The *h–p* version of the finite element method has been developed to analyze the vibration of membranes. This was accomplished using a polynomially enriched triangular element. New simple expressions of hierarchical C^0 shape functions for triangles were given in terms of the shifted Legendre orthogonal polynomials. In the *h–p* version of the finite element method, the accuracy of the solution is sought by simultaneously refining the mesh and increasing the polynomial order in each element. Results of frequency calculations for triangular and L-shaped membranes using a number of meshes and polynomial orders have illustrated the rapid convergence and high accuracy of the present method. In comparison to the linear triangular element, the triangular *p*-element was found to produce a higher accuracy with fewer degrees of freedom.

References

[1] I. Babuska, B. Guo, The *h–p* version of the finite element method, Part I: the basic approximation results, *Computational Mechanics* 1 (1986) 21–41.
[2] L. Demkowicz, J.T. Oden, W. Rachowicz, O. Hardy, Toward a universal *h–p* adaptive finite element strategy, Part I: constrained approximation and data structure, *Computational Methods in Applied Mechanics and Engineering* 77 (1989) 79–112.
[3] N.S. Bardell, J.M. Dunsdon, R.S. Langley, Free vibration analysis of thin rectangular laminated plate assemblies using the *h–p* version of the finite element method, *Composite Structures* 32 (1995) 237–246.
[4] N.S. Bardell, An engineering application of the *h–p* version of the finite element method to the static analysis of a Euler–Bernoulli beam, *Computers and Structures* 59 (1996) 195–211.
[5] A. Houmat, Hierarchical finite element analysis of the vibration of membranes, *Journal of Sound and Vibration* 201 (1997) 465–472.
[6] A. Peano, Hierarchies of conforming finite elements for plane elasticity and plate bending, *Computers and Mathematics with Applications* 2 (1976) 211–224.
[7] B. Szabo, I. Babuska, *Introduction to Finite Element Analysis*, Wiley, New York, 1989.
[8] M. Abramowitz, I.A. Stegun, *Handbook of Mathematical Functions*, Dover Publications, New York, 1965.
[9] P.M. Morse, H. Feshbach, *Methods of Theoretical Physics*, McGraw-Hill, New York, 1953.
[10] L. Fox, P. Herrici, C. Moler, Approximations and bounds for eigenvalues of elliptic operators, *SIAM Journal on Numerical Analysis* 4 (1967) 89–102.